Hosted by
Spain Water
and IWHR, China

27th IAHR International Symposium on Ice
Gdańsk, Poland, 9 – 13 June 2024

Experiments on Ice Load Reductions on Dams

Chris Petrich[1,2], Irina Sæther[1,2], Megan O'Sadnick[1], Bård Arntsen[1,2]

[1]SINTEF Narvik, Narvik, Norway
[2]Ice Mate AS, Norway
christian.petrich@sintef.no

Static ice loads are a significant aspect of the design of hydropower dams in Norway due to their low height. Results are presented from a preliminary study to investigate whether elastic foam could be used to reduce static ice loads. Frames with stress cells were mounted on the dam at Taraldsvikfossen reservoir near Narvik in the winter of 2016/17, with some frames covered by closed-cell elastic foam. Ice loads were due to thermal events and water level changes. In the presented measurements, the magnitude of stresses on foam-covered frames was typically 10% of the magnitude of the stresses at the reference frame.

Keywords: ice load, lake ice, dam, measurements

1. Introduction

Static ice loads form a significant contribution to the design load of dams of low height in cold climates. While the magnitude of static ice loads can be significant, the potential deflection can be quite limited. In the case of thermal ice loads, the deflection would be limited to the lateral thermal expansion of the ice cover, reduced by creep. This study was therefore to test in a field setting in Taraldsvikfossen Reservoir whether there is a potential for elastic foam to reduce stresses exerted onto a dam. The idea of using foam can be traced back to at least Michel (1970). The location was chosen due to the existence of a multi-year record of ice load measurements (e.g. Petrich et al., 2020).

Taraldsvikfossen Reservoir is a small (3400 m^2) drinking water backup reservoir fed by a creek (Taraldsvikelva) at 213 m elevation, 68.43678° N, 17.49856° E. The crown of the dam is 0.5 m above the nominal water level which is maintained by a spillway. As described elsewhere (e.g. Petrich et al., 2020), the typical ice thickness is between 0.5 and 1.0 m, and the ice is attached to the dam. Taraldsvikfossen Reservoir exhibits at least two different sources of ice stresses: thermal stresses in response to ice temperature changes, and mechanical in response to small (decimeter) water level fluctuations that typically coincide with partial flooding of the ice surface. The latter arises from a creek discharging into the reservoir while the ice cover is frozen to the spillway. Creek discharge while the ice cover is frozen to the spillway results in visible upward movement of the ice cover away from the dam. This results in the formation of several decimeters of superimposed ice at the dam.

2. Methods

The methods used in this work follow earlier work (Petrich et al., 2020). Arrays of four vertically arranged custom-designed oil-filled GeoKon 4850 stress cells were used to measure ice stress (Figure 1). Each cell measured internal temperature at the same vertical level as the pressure (Petrich et al., 2015). The space between its two rectangular steel plates (100 mm×200 mm) was filled with de-aired oil. A short tube connected the cell to a vibrating wire pressure transducer that also measured temperature with a temperature-dependent resistor. A water pressure gauge had been installed at the dam at 1.3 m water depth.

The stress cells were spaced 180 mm vertically. At installation, the upper-most cell (later referred to as cell 1) was above the water line to be able to detect stresses from superimposed ice, should that form. Cells were suspended on metal tape (cf. Petrich et al., 2015; Figures 1,2,3). Tapes were mounted on a metal frame of 0.8 m width, except at Station D where the tapes were attached directly to the dam. One frame without foam was mounted at the center of the dam (Station A) (cf. Figure 2). A frame with one 12.5 mm thick foam layer (Station B) was mounted 2 m away from this frame (measured center-to-center of the cells) with another frame with two 12.5 mm thick foam layer directly adjacent to this (Station C). This was followed by 200 mm wide Station D without foam, followed by a frame with two and one 12.5 mm thick foam layers, respectively (Stations E and F). Stations B and F had only one stress cell mounted at the height of the second cell from the top of the other Stations. The frames were attached to wooden blocks screwed to the top surface of the dam. The frames with closed-cell elastic polyurethane foam were weighted at the bottom to compensate for buoyancy. Stress and temperature data were recorded every 5 minutes together with water pressure and weather data.

Line loads were calculated at each station by adding the individual stresses and multiplying them with their vertical separation of 0.18 m.

Thermal stresses were modeled as laid out by Petrich et al. (2020). For this, the temperature history of each stress cell was used to drive the thermal load and creep model of Petrich et al. (2015). This method is not optimal since the temperature profile at the measurement stations may not be representative of the temperature profile through the ice cover.

In the period from 8 to 11 March 2017, tests were performed to measure ice loads during water level changes. For this, water level was temporarily lowered twice by up to 35 cm. Details of those tests were reported elsewhere (Foss, 2017).

Ice thickness, freeboard and snow depth were measured in transects perpendicular to the dam at the center of the reservoir at distances from the dam 0.1, 0.5, 1, 2, 5, 10, 15, 20, and 25 m on 21 Nov, 5 Dec, 20 Dec, 4 Jan, 16 Jan, and 6 March.

3. Results and Discussions

An ice cover started to form from 14 to 15 October 2016 and stayed in place for the reminder of the winter. On 28 October, instruments were deployed in the ice, which was approximately 13 cm thick black ice at the time.

Ice thickness was greater toward the center of the reservoir than near the dam. Ice thickness had reached 35 to 60 cm by 5 December 2016, 37 to 67 cm on 4 January 2017, and increased to 52 to 72 cm by 6 March 2017. On 4 January 2017 the ice was comprised of three layers at the center of the reservoir, beyond ca 15-20 m from the dam: two 5 cm thick ice layers above the bulk of the ice, separated each by 5 cm thick gaps of water. This indicates that ice temperature was homogeneous at 0 °C in that area during this time and that thermal ice loads could only have originated from ice closer to the dam. On several occasions during warm periods in December and January there was a gap observed during site visits between ice cover and dam, implying that ice loads could have to be transferred through the lower parts of the ice cover, only.

Small water level fluctuations in the reservoir were caused by a slow inflow of water into the reservoir when the ice was frozen to the spillway. These water level changes induced fractures in the ice that were a source of superimposed ice formation (cf. Petrich et al. 2020). The crack pattern early in the season revealed a crack between Station A on one side, and the remaining stations on the other side (Figure 4). While the significance of the cracks is not clear, they could contribute to an inhomogeneous distribution of loads along the dam, which is commonly observed (e.g. Taras et al. 2011; Petrich et al., 2015).

Figure 5 shows the air temperature and water pressure sensor data in conjunction with the line loads calculated for the individual stations, and Figure 6 shows the individual stresses and stress cell temperatures underlying those calculations. Stations B and F are not shown since they contained only one cell that behaved like Cells C2 and E2, respectively. For the purpose of presentation, we divide the season into 5 phases as indicated in the figures. For a start it is obvious that notable line loads were detected at Stations A and D while the stations with foam cover, Stations B, C, E, and F did not register loads. Loads at Station D were generally higher than at Station A. This was expected because Station D is directly surrounded by foam-covered frames and should therefore experience increased stress due to bridging. However, the near complete absence of loads at the foam-covered frames was unexpected.

In Phase 1, a load event is apparent during the air temperature rise on 12 November. Photos indicate that the ice surface slowly flooded from the East toward the dam. At Station A, the upper cell (A2) initially went into compression while the cell below (A3) was in tension. On 14 Nov the situation was reversed with A3 in compression and A2 slightly in tension. The magnitude of the stresses was 250 kPa. At foam-covered Stations C and E, stresses were registered in the cells at corresponding depths, albeit only around 25 kPa magnitude. Station C was in tension at C3 on 12 November, followed by compression in C2 on 15 November. At Station E, cell E2 was in compression from 10 to 15 November while cell E3 was in tension. The net load at Station A was 50 kN/m. At Station D the peak stress reached 950 kPa on 12 November. From 11 until 13 November cell D2 was in compression, while from 13 until 14 November cell D3 was in compression with D2 in tension, and from 14 until 15 November D2 was in compression with D3 in tension. During the same time, the water pressure sensor indicated pressure fluctuations. The differential stresses registered between the second and third sensors are therefore most likely indicative of bending of the ice cover. Stresses at Station D were higher than at Station A presumably because the force from a larger area of the ice was transferred onto the dam through a narrow gap (bridge) between the foam frames.

In Phase 2, a peak load of 68 kN/m was registered at Station A on 23 November. The thermal ice load model predicted alternating tension and compression from 22 to 27 November, which is mirrored in the load at Station A, albeit at a higher magnitude than predicted (predicted magnitude was 16 kN/m). This difference could well be due to the ice temperatures near the wall not being representative of the ice temperatures across the reservoir. Interestingly, the measured load is almost entirely due to stresses in cell A3 while the predicted load is due to stresses calculated for cell A2. On 27 November the ice appears to add a bending component as the stress in A2 increases at the same rate the stress in A3 decreases. A second event in phase 2 from 4 to 5 December showed compression in A3 and to a smaller extent tension in A2, again indicating a bending component superimposed on a net ice load. With the exception of 27 November and 4 December, the stress development at Station A was not mirrored at Stations C, D, and E. After loads were registered from 21 to 22 November, the ice was generally in tension, except around 2 December when it was in compression. On 27 November and 4 December, sensor D3 registered stress development similar in shape and magnitude to sensor A3. While the peak line load at Station A was 68 kN/m during this phase, the line loads at foam-covered Stations C and E were <5 kN/m.

In Phase 3, the steep increase in air temperature on 5 January is not reflected in the ice stress data. At Station A, ice temperatures were with -1 °C close to the melting point already. At Stations C, D, and E, the bottom-most cell was frozen in and produced a load from 15 to 27 January. While the stresses at foam-free station A reached 125 kPa around 13 January, they were <10 kPa at foam-covered stations C and E.

In Phase 4, from 8 until 11 January, the data in the bottom-most two cells of Stations A and D appear to show oscillations with a period of ca 30 minutes (ranging from 20 to 60 minutes) with cell 3 going into compression while cell 4 goes into tension. From the end of 11 February through 13 February, cell A2 behaves anticyclic to cell A4 at Station A, while the signal disappears from D4 from 12 February. The highest stress of 990 kPa was recorded in cell D2 on 11 February. The measured line load at Station D on 11 and 12 February matches the predicted thermal line load from the temperature measurements (approximately 100 kN/m), while the net line load at Station A is slightly negative at this time, contrary to expectations based on local ice temperature. A similar situation had been reported by Petrich et al. (2015). Stress signals at Stations C and E during this phase resemble each other, bearing no obvious relation to the signals at Stations A and D. At Stations C and E from 1 to 6 February, cell 2 goes into compression, then tension as cell 3 goes into compression, which enters tension as cell 4 goes into compression. The stress magnitude is 17 and 25 kPa at Station C and E, respectively.

In Phase 5, ice load tests were performed by lowering and increasing the water level in the reservoir by up to 35 cm (Foss, 2017). While ice loads registered at Station D were between 50 and 100 kN/m since 6 March, they fell to zero abruptly at the beginning of the tests on 8 March only to re-appear at the end of the tests on 10 March. It may be assumed that some form of crack formation was responsible for this. Station A recorded loads predominantly during water level changes, reaching up to 85 kN/m. Foam-covered Stations C and E registered stresses in the bottom-most cell 4 while the water level was lowest, at magnitudes of 50 and 25 kPa, respectively.

While line loads reached 68 kN/m at Station A before the water level tests and 83 kN/m during those tests, line loads at foam-covered Stations C and E were always less than 10 kN/m. However, ice bridge Station D, between foam-covered Stations C and E, exceeded 100 kN/m on several occasions, with a maximum load of 180 kN/m registered. The reason for the low loads at Stations C and E was probably a combination of load reduction due to the foam and load transfer into the ice bridge instrumented by Station D. While the local load at Station D was high, the area-averaged load across two foam-covered frames of 0.8 m width and the gap of 0.2 m width would thus have been <30 kN/m, which is less than half of the loads observed at reference Station A.

4. Conclusions

Ice loads on a dam were measured in the winter 2016/17 using load cells that were either exposed to the ice or covered with foam. In this investigated winter there were few load events that could be attributed to thermal ice loads while indication of bending moment at the dam were rather common. The recorded stress signals differed between measurement stations, corroborating earlier assessments that the stress is typically not homogeneous along the length of the dam. The magnitude of the stresses at the foam-covered Stations C and E was 10% of exposed Station A, indicating that a foam cover holds promise as an option to reduce ice loads onto dams. Station D, forming a narrow bridge between Stations C and E, registered stresses two to four times the magnitude of reference Station A. The foam was clearly effective at reducing ice loads locally and an assessment of the reduction potential of the global load onto the dam should be performed.

Acknowledgements

This work was supported by the Research Council of Norway project number 195153 (ColdTech) with additional support from Statkraft and NVE. The support of Tore Pettersen during the field measurements is gratefully acknowledged.

References

Foss, A.B., 2017. Islast mot dammer med varierende vannstand. (Ice loads on dams during changing water levels.) M.Sc. Thesis, NTNU, Norway, 126 pp.

Michel, B. (1970). Ice Pressure on Engineering Structures. Cold Regions Science and Engineering Monograph III-B1b, CRREL, New Hampshire, 80pp.

Petrich, C., I. Sæther, L. Fransson, B. Sand, B. Arntsen, 2015. Time-dependent spatial distribution of thermal stresses in the ice cover of a small reservoir. Cold Regions Science and Technology, 120, 35–44. https://dx.doi.org/10.1016/j.coldregions.2015.09.003

Petrich, C., I. Sæther, M. O'Sadnick, and B. Arntsen, 2020. Static ice loads on a dam in a small Norwegian reservoir. In Proceedings of the 25th IAHR International Symposium on Ice, Trondheim, 23-25 Nov 2020, 16pp.

Taras, A., Côté, A., Comfort, G., Thériault, L., Morse, B., 2011. Measurements of ice thrust at Arnprior and Barrett Chute dams. Proceedings of the 16th Workshop on the Hydraulics of Ice-Covered Rivers, Winnipeg, MB, Canada, 18–22 September 2011, pp. 317–328.

Figures

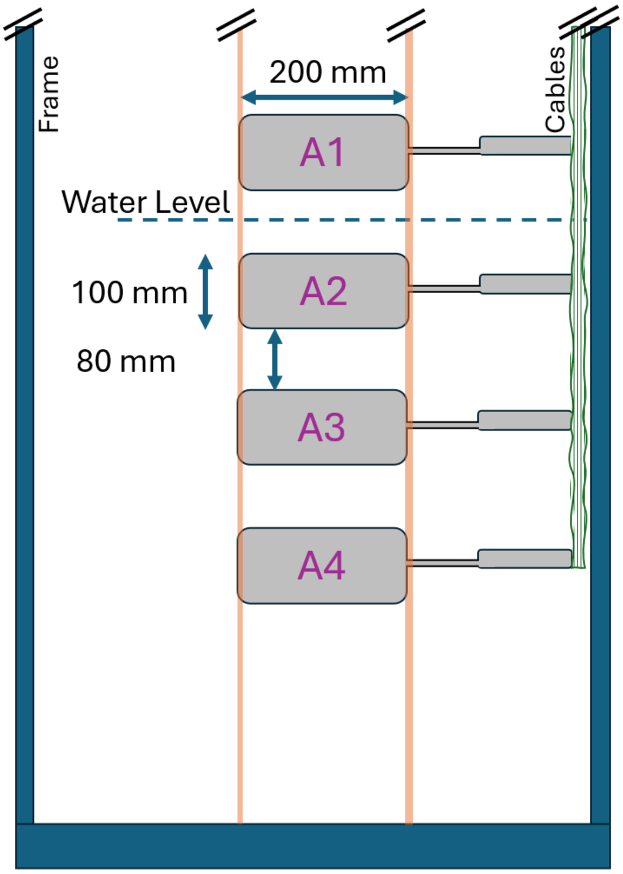

Figure 1. Vertical arrangement of cells and naming convention of the stress cells at Stations A, C, D, and E. Stations B and F had only one cell at a vertical level equivalent to A2. The top-most cell (e.g., A1) was mounted above the original water level to capture any superimposed ice. Station D did not have a frame.

Figure 2. Photograph of the Station layout in 2016/17 after installation on 28 Oct 2016. Note that frames, foam (pink) and cells are reflected on the ice surface. Letters label the corresponding measurement stations.

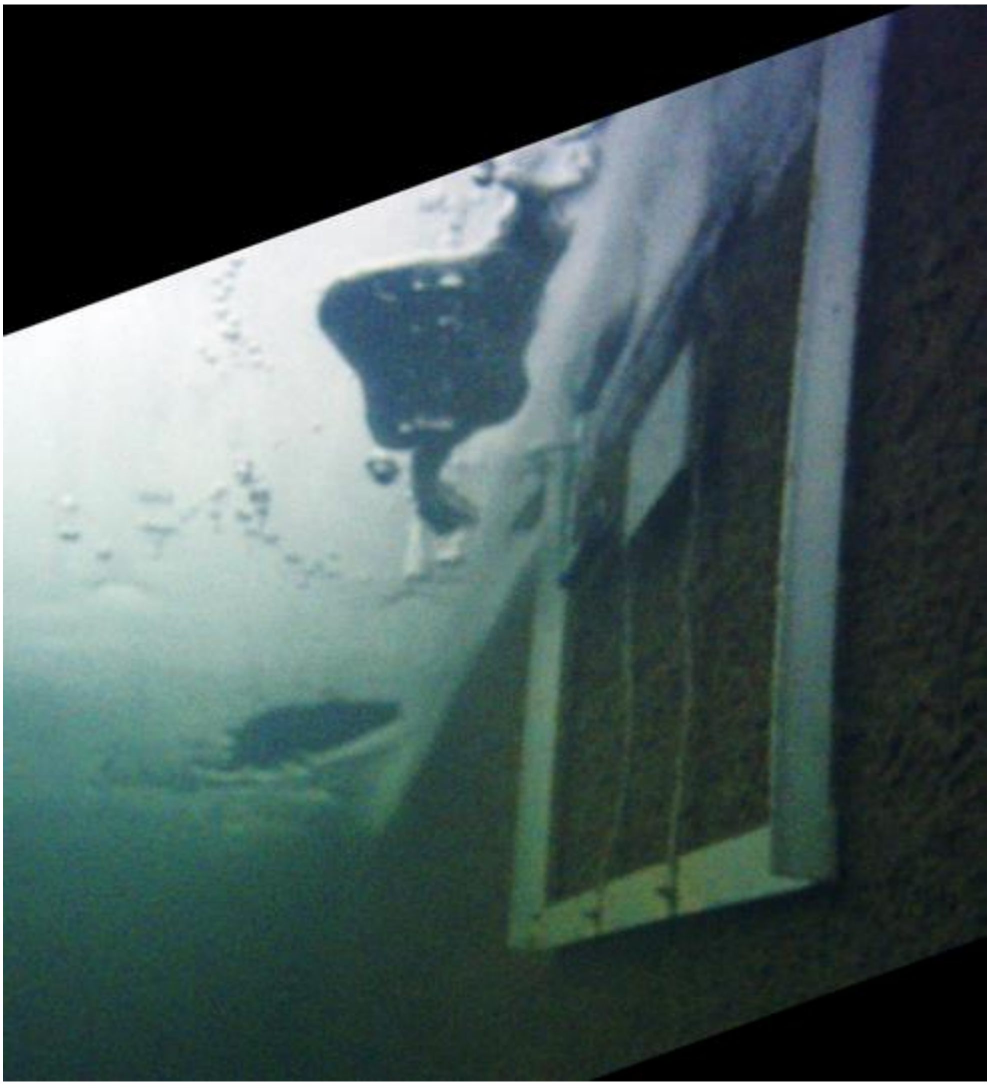
Figure 3. Underwater photo of Station A on 4 February 2017. Visible are the metal tapes holding the cells to the frame, and the bottom-most cell beneath the ice cover.

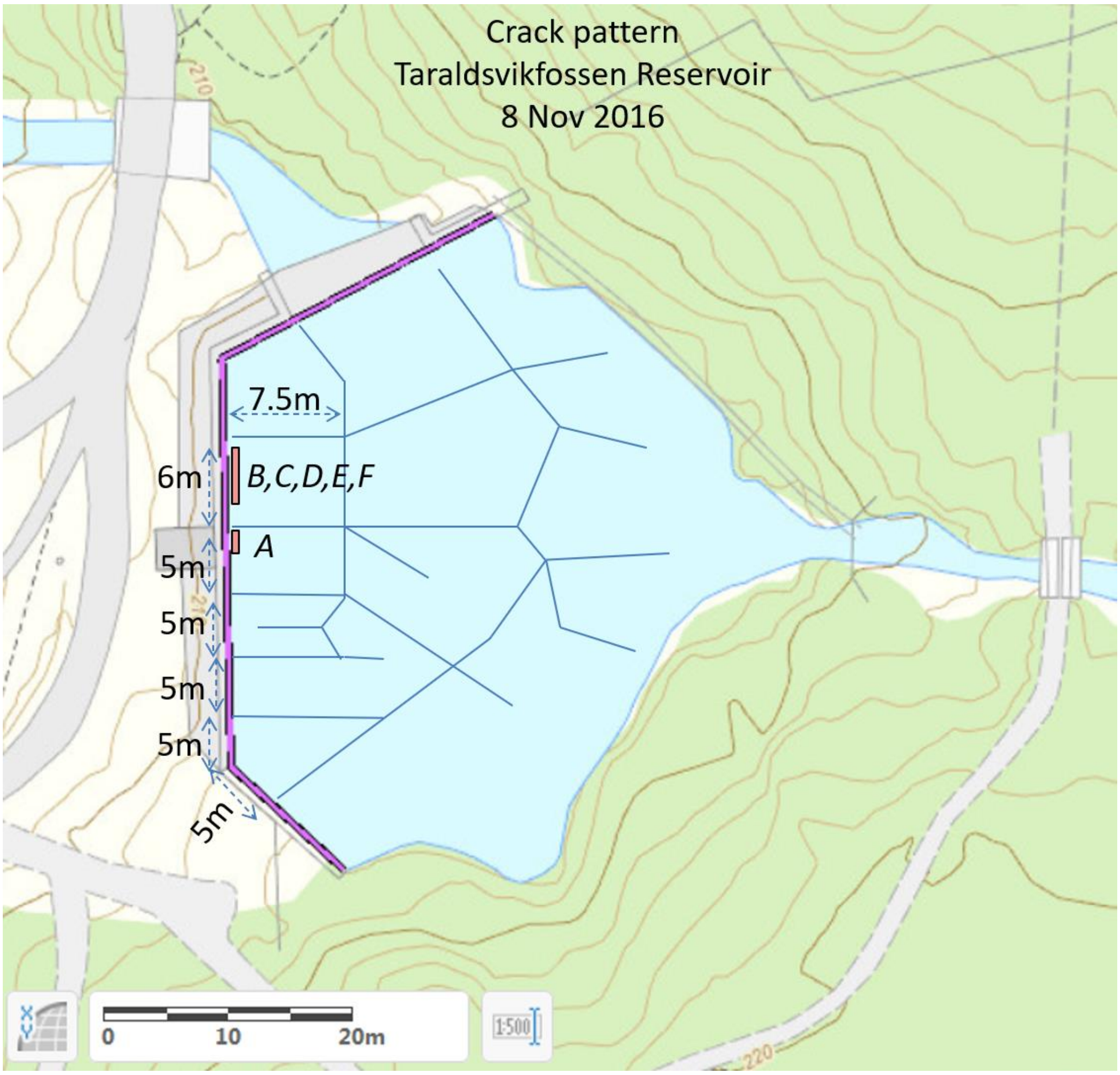

Figure 4. Crack pattern in the reservoir visible on 8 Nov 2016 (blue lines). Note that one crack separates Station A (south) from Stations B,C,D,E, and F (north). Base map: https://atlas.nve.no/

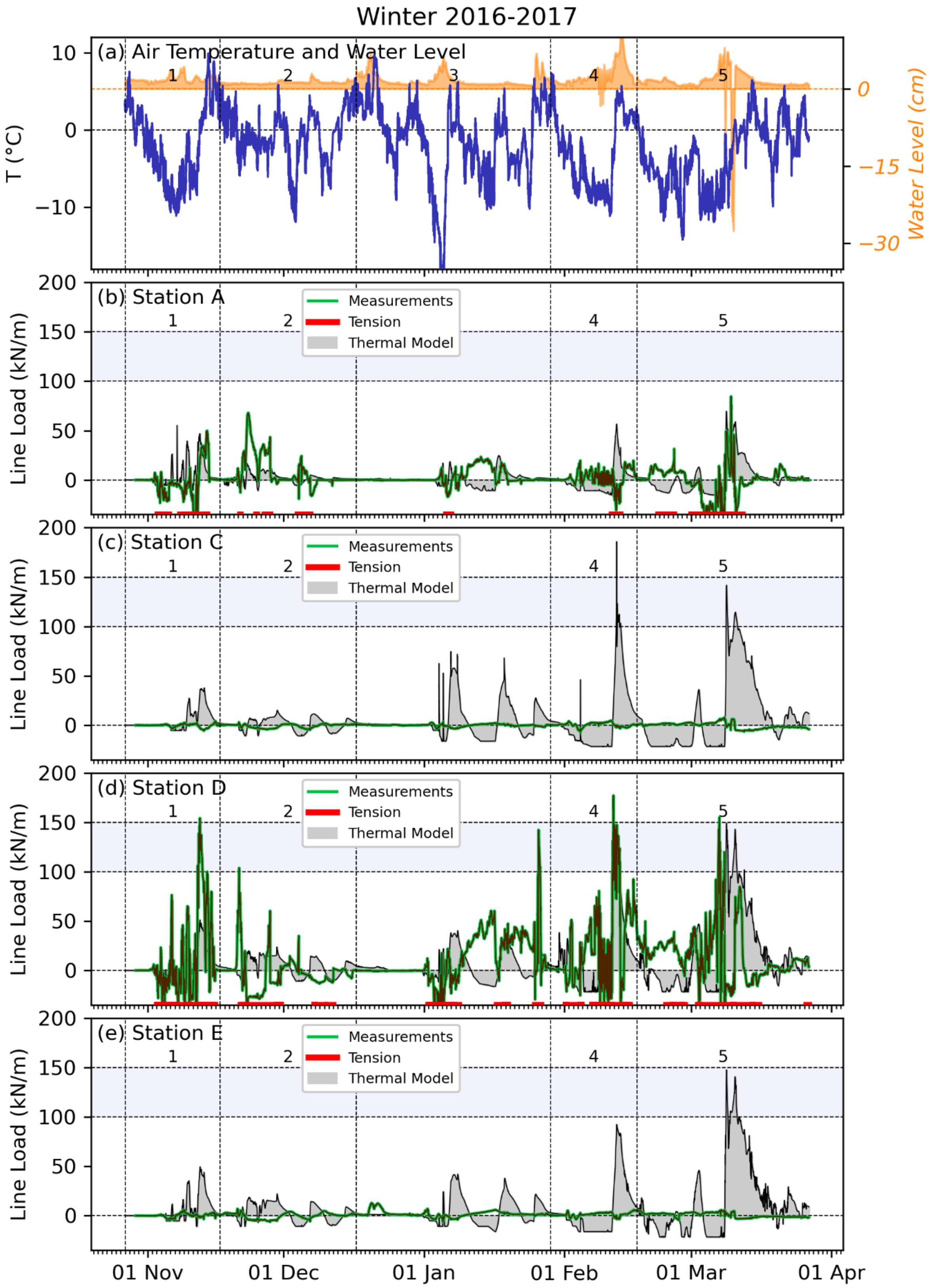

Figure 5. Air temperature and water pressure (a), and measured line loads and calculated thermal line loads at Stations A (b), C (c), D (d), and E (e).

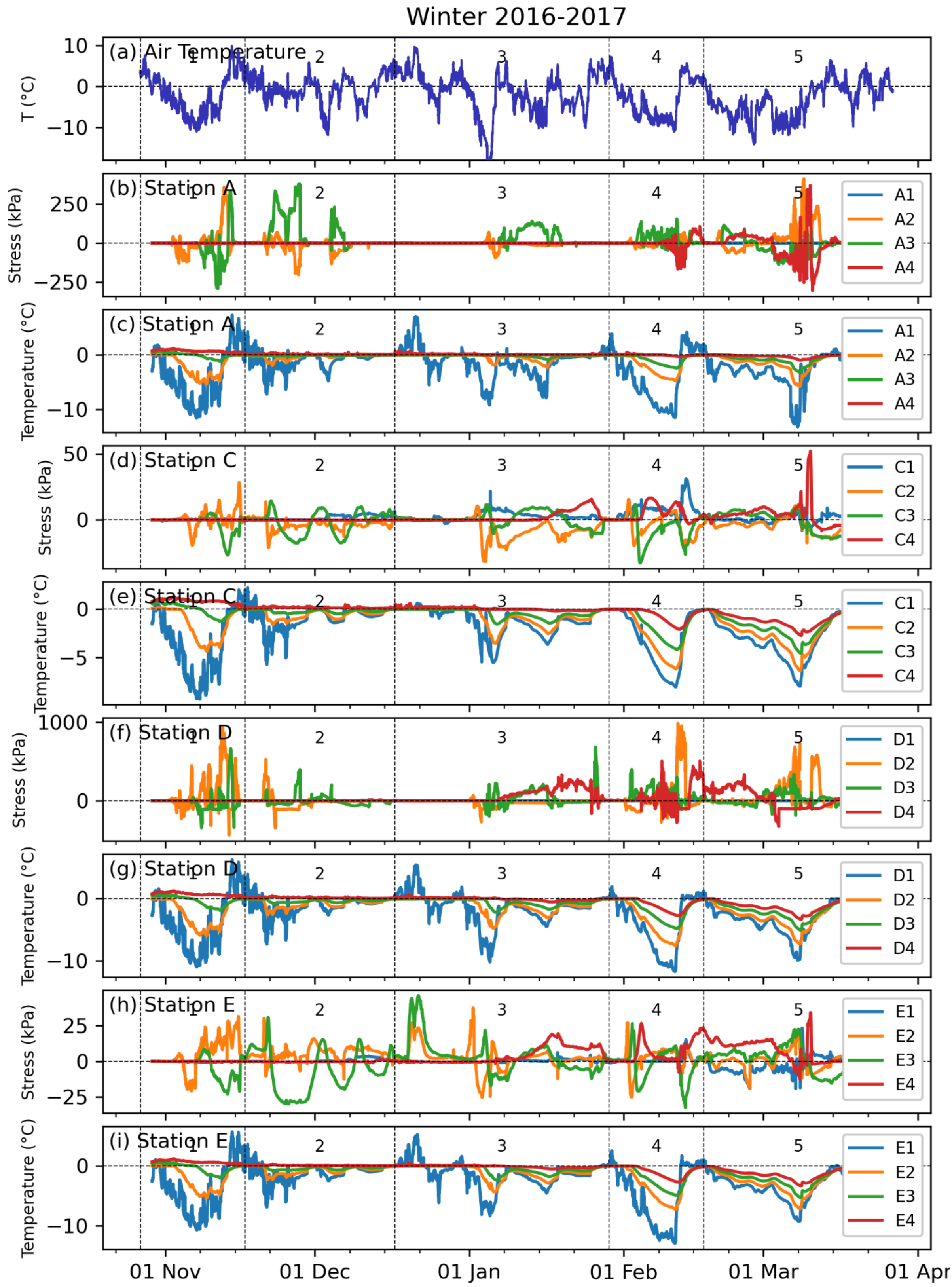

Figure 6. (a) Air Temperature, and (b,d,f,h) stress and (c,e,g,i) temperatures recorded by individual stress cells. Cell number 1 was positioned above the initial ice surface, and cell number 4 was at the bottom. Note difference in scales.